NASA Technical Paper 1183

A Distributed Vortex Method for Computing the Vortex Field of a Missile

Raymond L. Barger

JUNE 1978

NASA

NASA Technical Paper 1183

A Distributed Vortex Method for Computing the Vortex Field of a Missile

Raymond L. Barger
Langley Research Center
Hampton, Virginia

National Aeronautics
and Space Administration

**Scientific and Technical
Information Office**

1978

SUMMARY

Vortex sheet development in the flow field of a missile was investigated by approximating the sheets in the cross-flow plane with short straight-line segments having distributed vorticity. In contrast with the method that represents the sheets as lines of discrete vortices, this distributed vortex method produced calculations with a high degree of computational stability.

INTRODUCTION

The vortex sheets that are shed from the wings of large airplanes have recently been the subject of extensive study because of the potential hazard to other aircraft that encounter the wake vorticity. (See, for example, ref. 1.) The vortex field around a missile, on the other hand, is of interest because of its influence on the stability and control of the missile itself. (See ref. 2.) This vortex field has been extensively studied by tracking the vorticity in successive cross-flow planes. This slender-body approximation requires only that flow variations be gradual in the axial direction; therefore, it is applicable for describing the external flow field even at high angles of attack where slender-body theory is not valid for computing the surface velocities. Thus, from the standpoint of computing the flow field, the missile surface is looked on primarily as a generator of vorticity.

The actual problems associated with obtaining the locations and strengths of the incipient vorticity arising from the nose, the forward fins, and the afterbody (fig. 1) have been treated in a number of studies conducted by Nielsen Engineering and Research, Inc. (See ref. 3 and its references.) Fidler's method (ref. 4) for treating the afterbody vorticity is reviewed briefly in the present paper because the method is applied here to a continuous emission of vorticity; consequently, some of the equations assume a slightly different form from those in reference 4, which treats discrete vortices. One problem that has not yet been completely resolved is that of obtaining an accurate spanwise loading distribution for the canard region in the presence of separated flow from the body surface ahead of the canard trailing edge.

Heretofore, the vortex field has been treated either by assuming that the roll-up is complete from incipience (ref. 3) or by approximating the vortex sheet, which occurs as a line in the cross-flow plane, as an array of discrete vortices (ref. 1). The former method possesses the advantages of simplicity and rapidity of calculation, but it is accurate only when the vorticity is highly concentrated. The latter method, on the other hand, tends to become unstable because the mathematical singularities representing two vortices in close proximity give values too large for the velocities induced by the vortices on each other. If the problem is avoided by combining the two vortices into a single strong vortex, a new problem is introduced: a vortex on one segment of the roll-up spiral can join with a vortex on an adjacent segment. (See fig. 2(a).) The result is a spurious distortion of the spiral by the strong

combined vortex. Other attempts to avoid the roll-up instability of discrete vortices employ arbitrary parameters that could lead to violation of the conservation equations. (See ref. 1.)

Another approach to the problem of calculating the vortex sheet roll-up is to represent the sheets with straight-line segments in the cross-flow plane; the algebraic singularity is thereby reduced to a logarithmic singularity. (See fig. 2(b).) This method has been applied to roll-up in the presence of wind-tunnel walls (ref. 5) and has exhibited a high degree of stability.

In the present investigation, the approach of reference 5 has been applied to the problem of calculating the development of vortex sheets emitted from the wing and body surfaces of a missile. This procedure has been computerized and may ultimately be incorporated into other computer programs to improve the prediction accuracy of surface pressure and force calculations.

However, the immediate usefulness of the method is deemed to be the interpretation of vapor screen pictures. Suppose, for example, that the computed wing spanwise loading distribution leads to a calculated shape for the vortex sheet that does not resemble the vortex sheet observed experimentally. This result would indicate that the forward wing-body section was not performing in accordance with the intent of its design. Furthermore, if, by experience, a loading distribution were known that would produce a computed sheet that did resemble the vapor screen result, then the form of that distribution would provide insight into the nature of the discrepancy (as, for example, the location and extent of a separated flow region).

SYMBOLS

F_B net flux of vorticity per unit time flowing from body surface at separation line

M Mach number

R radius of missile cross section

r complex coordinate of field point in missile cross-flow plane, $y + iz$

U circumferential velocity at boundary-layer edge

V free-stream velocity

w complex disturbance velocity

$\tilde{w}$ complex disturbance velocity due to image of a vortex

w_{kj} complex velocity in cross-flow plane at r_k due to vortex line extending from ρ_j to ρ_{j+1}

$\tilde{w}_{kj}$ complex velocity in cross-flow plane at r_k due to image of vortex line extending from ρ_j to ρ_{j+1}

x distance along missile axis

α angle of attack

Γ vortex strength

γ vortex density function

θ angular coordinate on body cross section measured from windward side

Λ proportionality constant (see eq. (7))

ρ complex coordinate of discrete vortex in missile cross-flow plane, $\eta + i\zeta$

$\tilde{\rho}$ image of ρ in circle representing body cross section

χ scalar distance in cross-flow plane

Subscripts:

j,k indices referring to jth and kth line segments, respectively

s at separation line

Superscript:

$*$ complex conjugate

ANALYSIS

The simplifications of the slender-body theory, which are assumed in this study, permit the flow development to be described by two-dimensional calculations in the time-dependent cross-flow plane. Straight-line segments are used to approximate each continuous lateral vortex sheet. (See fig. 3.)

In the notation of reference 5, the complex velocity in the cross-flow plane at a point r, due to a unit strength vortex at ρ, is

$$w = \frac{i}{2\pi} \frac{1}{r - \rho} \tag{1}$$

The velocity induced at r_k by a short straight segment, from ρ_j to ρ_{j+1}, of the line of vorticity is therefore (fig. 3)

$$w_{kj} = \frac{i}{2\pi} \int_{\rho_j}^{\rho_{j+1}} \frac{\gamma}{r_k - \rho} \, d\chi \tag{2}$$

where γ is the vortex density function and

$$d\chi = |d\rho| = \sqrt{d\eta^2 + d\zeta^2}$$

The increment $d\chi$ can be written

$$d\chi = \frac{d\rho\, d\rho^*}{|d\rho|} = \frac{\left(\rho^*_{j+1} - \rho^*_j\right) d\rho}{|\rho_{j+1} - \rho_j|}$$

or alternatively

$$d\chi = \frac{(\rho_{j+1} - \rho_j)\, d\rho^*}{|\rho_{j+1} - \rho_j|}$$

Consequently, from equation (2),

$$w_{kj} = \frac{\gamma_j i}{2\pi} \frac{\rho^*_{j+i} - \rho^*_j}{|\rho_{j+1} - \rho_j|} \log \frac{r_k - \rho_{j+1}}{r_k - \rho_j} \tag{3}$$

where γ_j is assumed constant over the line segment.

In reference 5, the velocity field included the velocity due to images representing the effect of straight wind-tunnel walls. In the present problem, images are required to satisfy the condition at the circular boundary of the missile body in accordance with the circle theorem. In reference 3, the authors have observed that the only images to be used are those required to satisfy the boundary condition on the missile surface. They note that the vortex that is normally inserted at the center of the circle in two-dimensional calculations in order to satisfy a circulation condition at infinity must be omitted because there is no circulation at infinity. The velocity in the cross-flow plane induced at r by the image of a unit vortex at ρ is

$$\tilde{w} = \frac{i}{2\pi} \frac{1}{r - (R^2/\rho^*)} \tag{4}$$

Let

$$\tilde{\rho} = a^2/\rho^*$$

Then the velocity at r_k, due to the image associated with the vorticity on the line segment from ρ_j to ρ_{j+1}, is

$$\tilde{w}_{kj} = \frac{\gamma_j i}{2\pi} \frac{\tilde{\rho}_{j+1} - \tilde{\rho}_j^*}{\left|\tilde{\rho}_{j+1} - \tilde{\rho}_j\right|} \log \frac{r_k - \tilde{\rho}_{j+1}}{r_k - \tilde{\rho}_j} \tag{5}$$

The total induced velocity at point r_k is obtained by summing contributions of the type given by equations (3) and (5) as follows:

$$w(r_k) = \tilde{w}_{kk} + \sum_{j \neq k} \left(w_{kj} + \tilde{w}_{kj}\right) \tag{6}$$

For computing the development of the vortex sheet, the points r_k are taken at the midpoints of the segments making up the sheet.

The complex logarithm functions in equations (3) and (5) require somewhat more calculation time than the concentrated vortex expressions (eqs. (1) and (4)); therefore, the latter expressions are used when the distance from the vortex to the observation point is large enough to justify the use of the approximation. Normally, this distance is on the order of the body radius.

If Δx denotes the distance between the intersections of successive cross-flow planes with the missile axis, then the incremental movement of a coordinate of the vortex sheet is given by

$$\Delta\rho_j = w_j \frac{\Delta x}{V \cos \alpha}$$

where w_j, the velocity at ρ_j, is obtained by interpolating the velocities computed at the midpoints of the segments. Thus, the coordinates defining the vortex sheet in the next cross-flow plane are given by $\rho_j + \Delta\rho_j$.

Although the development of the vortex sheet has been the primary subject of interest in these calculations, the velocity induced by the sheet at any point in the cross-flow plane can be obtained from equation (6).

An initial distribution of vorticity is required to start the calculation. For forward fins that support a loading, the vorticity at the trailing edge is obtained by the usual method of differentiating the spanwise loading distribution. In the present investigation, the calculation was started at the trailing edge of the forward fin with the nose vorticity either neglected, assumed,

or estimated. However, either the method of reference 3 or the recently available method of reference 6 can be used to obtain the starting conditions for the nose vortices.

When flow separation from the body surface occurs, the resulting vortex sheet can be computed with the use of an approximate procedure of the type developed by Fidler (ref. 4). According to reference 4, the net flux of vorticity flowing from the body surface per unit time F_B is given by the following equation:

$$F_B = \Lambda \int_0^x \frac{U_s^2}{2} \, dx \tag{7}$$

where, by a two-dimensional analogy type of argument, $\Lambda \sim 1/2$ and U_s is related to θ_s, the angular coordinate of the separation line, by

$$U_s = V \sin \alpha \sin \theta_s$$

The term "two-dimensional analogy" is used because the use of the two-dimensional cross-flow analysis is applicable only to the inviscid flow. A complete boundary-layer analysis would involve a three-dimensional calculation, including a consideration of the influence on surface pressure of the off-surface vorticity already existing in the missile flow field. Therefore, the Fidler approach was adopted, although it requires the use of empirical data, that is, the value of θ at which separation occurs.

The effect of the vorticity emitted from the body surface is calculated by introducing into the flow field at periodic intervals a line segment extending from the separation line to the point that was last emitted from the surface. The total vortex strength for the segment, according to equation (7), is $\Lambda \frac{U_s^2}{2} \frac{\Delta x}{V \cos \alpha}$. This expression is obtained by integrating over an axial distance Δx and dividing by the axial component of velocity.

The actual computer time required for the calculation of the sheet roll-up depends on the number of sheets included in the calculation and the number of x-stations required for the calculation. Symmetry about the ζ axis reduces the computer time by approximately one-half. Typical computational times for physically symmetric examples, computed on a Control Data CYBER 175 computer system, range from 1 to 3 minutes.

When the vortex sheets are treated as fully developed discrete vortices from inception, the computing time is small: always less than 10 seconds on the Control Data CYBER 175 computer system, even if several vortices are involved. Since this approximation has been extensively used and the computational time is so short, the first two examples of the following section

include the locations of the discrete vortex representations of the corresponding vortex sheets for purposes of comparison.

EXAMPLES AND DISCUSSION

The first two examples are designed to demonstrate the application of the discrete vortex method in a field containing four distinct vortex sheets and to illustrate some features of the sheet development that are lost when the trailing vorticity is represented as concentrated vortices. The example shown in figure 4 describes one stage in the development of the vortex sheets behind the forward fins of a cruciform missile at a roll angle of 45° and an angle of attack of 0°. The vortex sheets are associated with the lift produced by deflecting the fins. Figure 4(a) shows the straight vortex sheets in their initial positions with the vortex strength distribution indicated by the shaded area along one of the sheets.

Figure 4(b) shows the developing vortex sheets. As the outer sections of the sheets begin to roll up into tip vortices, the inner sections of the sheets move clockwise on the right side of the body surface and counterclockwise on the left. This movement results from the velocity field of the image vortices in the body cross section.

The second example (fig. 5) is similar to the first except that the missile is set at a small positive angle of attack (10°). For this example, the inner edges of the vortex sheet move more generally upward, in contrast to the first example, because the effect of the image vortices is counteracted by the acceleration of the vertical cross flow near the missile body.

The third example (fig. 6) illustrates the development of vortex sheets resulting from lifting canard surfaces in the presence of vorticity emitted from the nose section. Afterbody vorticity is omitted in this example. The calculation is initiated near the canard trailing edge. The initial length and vorticity distributions of the sheets were estimated to be similar to those of a conventional Sparrow-type missile without roll and at an angle of attack of 27°. The shape of the vortex sheet in the cross-flow plane 2 body diameters downstream of the canard trailing edge is shown in figure 6(a).

An attempt was made to compare the calculated shape in figure 6(a) with the vortex sheet of a Sparrow-type missile observed in a vapor screen photograph. This missile is a conventional type with a circular body and cruciform wing and tail. (See ref. 7 for actual dimensions.) The missile was tested without roll at an angle of attack of 27°, and at a Mach number of 3.95.

Many difficulties arise in making a comparison with such a record. The vapor screen camera was set outside the tunnel with the line of sight set at approximately 45° to the free-stream flow. Consequently, distances taken from the photograph had to be altered to compensate for the camera angle. The illuminated plane intersected the missile axis at the same location as the cross-flow plane shown in figure 6(a), but the vapor screen plane is vertical rather than normal to the missile axis. Other problems involved in making the comparison include the nebulous nature of the vortex sheet observed experimentally

and the aforementioned uncertainity in estimating the spanwise wing loading in the presence of nose vortices. The estimated form of the vortex sheets taken from the vapor screen picture is shown in figure 6(b), and it compares qualitatively with the calculated shape of figure 6(a).

An example in which vorticity arising from the afterbody plays a major role is shown in figure 7(a). The missile configuration and test conditions are the same as in the previous example except that the angle of attack is 33°. At this high angle of attack, the afterbody vortices are quite strong and have a major effect on the fin forces. Therefore, in this example the afterbody vorticity was included in the calculation with the result shown in figure 7(a) for the cross-flow plane 5 body diameters downstream of the wing trailing edge. The corresponding vapor screen shape is shown in figure 7(b). The comparison, which is subject to the same limitations discussed in the previous example, nevertheless displays a definite similarity of form.

CONCLUDING REMARKS

The development of vortex sheets in the flow field of a missile has been studied by approximating the sheets in the cross-flow plane with short straight-line segments having distributed vorticity. In contrast with the method that represents the sheets as lines of discrete vortices, the distributed vortex method resulted in a high degree of computational stability for the roll-up process. The primary shortcoming of this method is that it requires significantly more computer time than the method of discrete vortices.

Langley Research Center
National Aeronautics and Space Administration
Hampton, VA 23665
April 24, 1978

REFERENCES

1. Rossow, Vernon J.: Survey of Computational Methods for Lift-Generated Wakes. Conference on Aerodynamic Analyses Requiring Advanced Computers, Part II, NASA SP-347, 1975, pp. 897-923.

2. Sawyer, Wallace C.; Jackson, Charlie M., Jr.; and Blair, A. B., Jr.: Aerodynamic Technologies for the Next Generation of Missiles. Paper presented at the AIAA/ADPA Tactical Missile Conference (Gaithersburg, Maryland), Apr. 27-28, 1977.

3. Nielsen, J. N.; Hemsch, M. J.; and Dillenius, M. F. E.: Further Studies of the Induced Rolling Moments of Canard-Cruciform Missiles as Influenced by Canard and Body Vortices. NEAR TR 79 (Contract No. N00123-74-C-0829), Nielsen Eng. & Res., Inc., Jan. 31, 1975.

4. Fidler, John E.: Approximate Method for Estimating Wake Vortex Strength. AIAA J., vol. 12, no. 5, May 1974, pp. 633-635.

5. Mokry, M.; and Rainbird, W. J.: Calculation of Vortex Sheet Roll-Up in a Rectangular Wind Tunnel. J. Aircr., vol. 12, no. 9, Sept. 1975, pp. 750-752.

6. Spangler, Selden B.; and Mendenhall, Michael R.: Further Studies of Aerodynamic Loads at Spin Entry. Rep. ONR-CR212-225-3, U.S. Navy, June 30, 1977. (Available from DDC as A047 952.)

7. Monta, William J.: Supersonic Aerodynamic Characteristics of a Sparrow III Type Missile Model With Wing Controls and Comparison With Existing Tail-Control Results. NASA TP-1078, 1977.

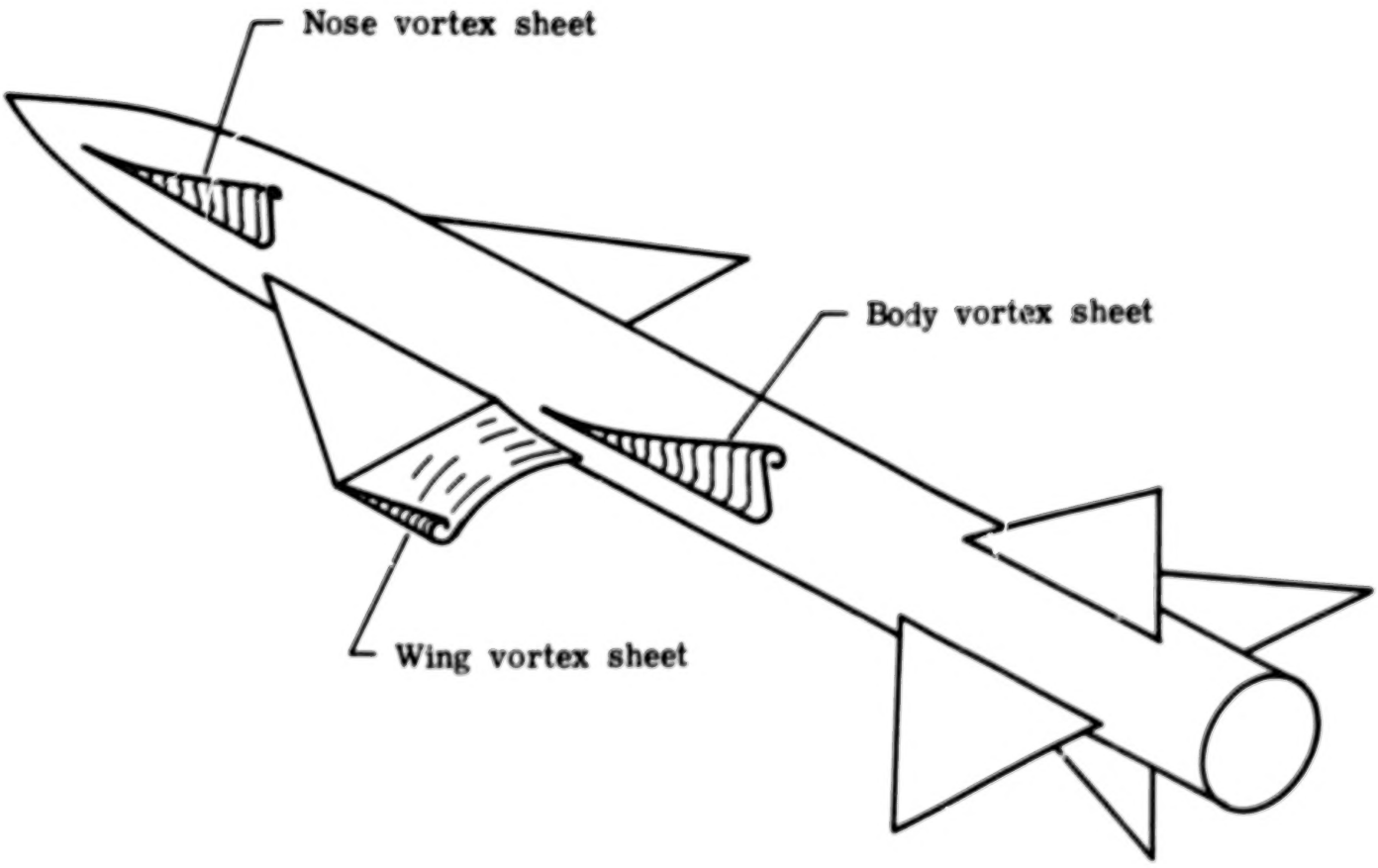

Figure 1.- Sketch showing vortex sheets emitted from nose, wing, and afterbody regions.

(a) Discrete vortex method. The strong vortex formed by combining two vortices causes large local velocities that disrupt the roll-up process.

(b) Distributed vortex method. Absence of large local velocities permits the sheet to roll up smoothly.

Figure 2.- Comparison of vortex sheet representations as discrete vortices and as distributed vortices.

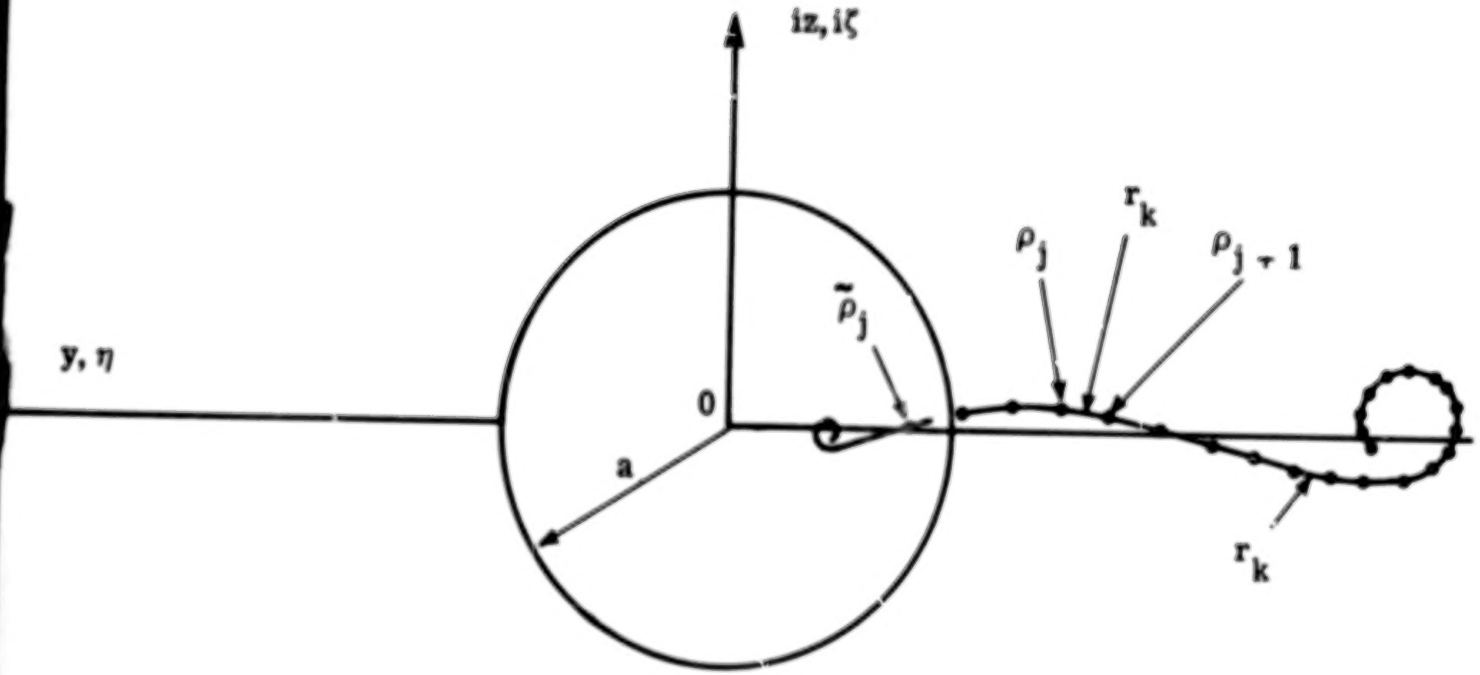

Figure 3.- Vortex sheet geometry in missile cross-flow plane.

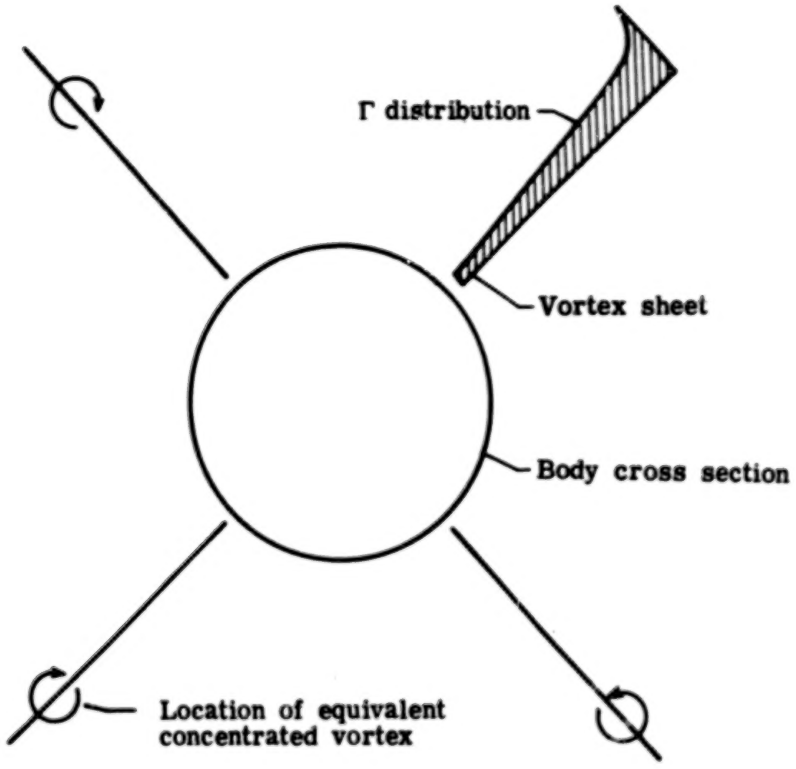

(a) Initial form of vortex sheets and vortex strength distribution.

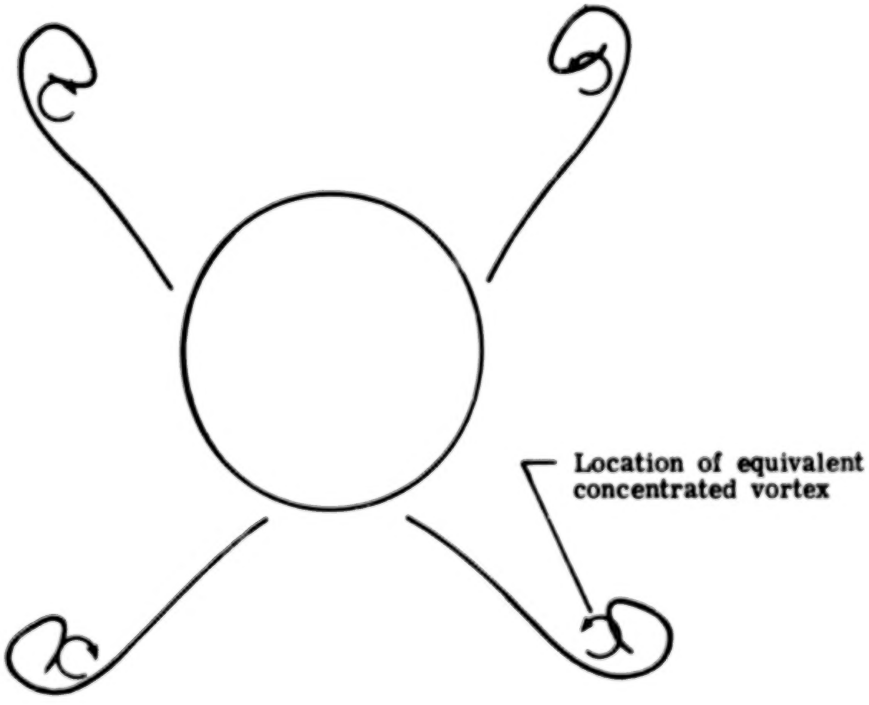

(b) Developing vortex sheets.

Figure 4.- Vortex sheet development for cruciform missile with deflected forward fins at roll angle of 45° and angle of attack of 0°.

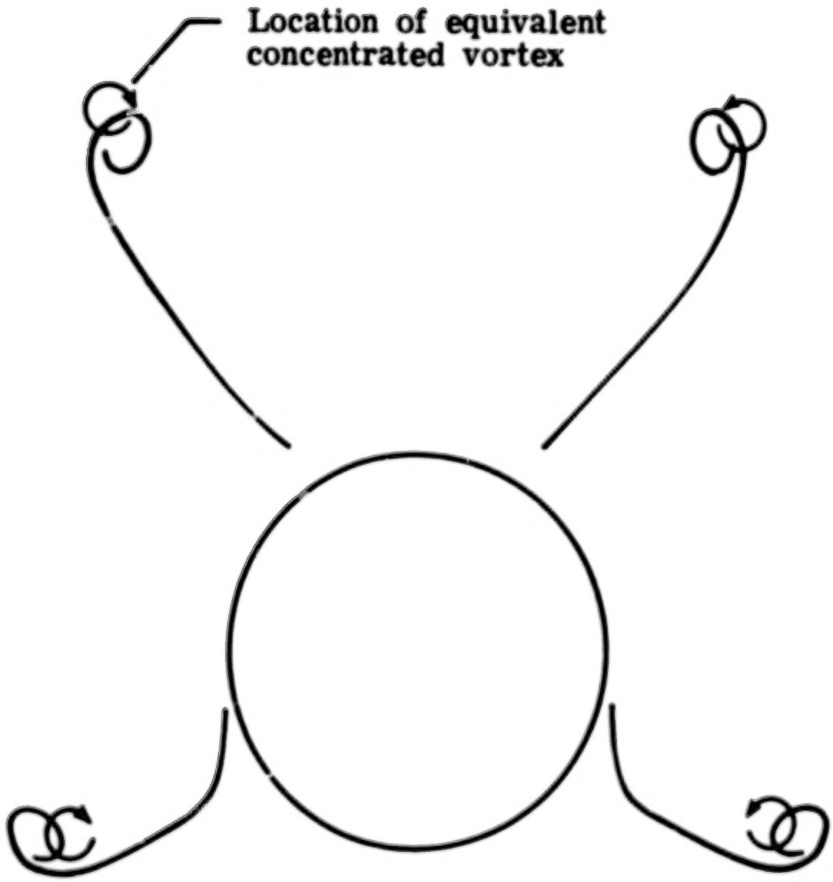

Figure 5.- Developing vortex sheets for cruciform missile with deflected forward fins at roll angle of 45° and angle of attack of 10°.

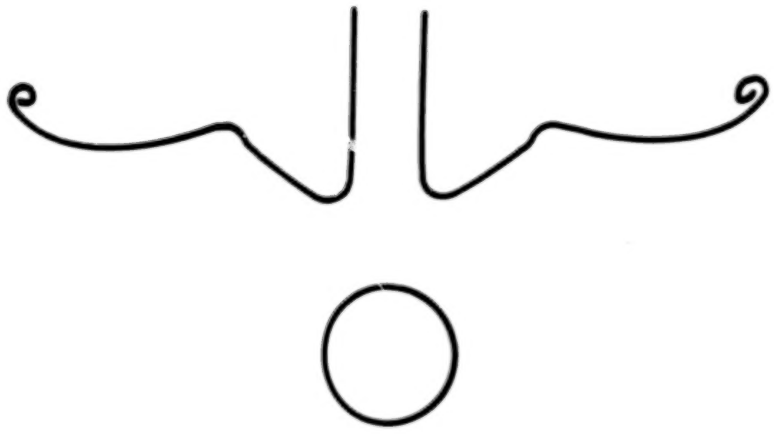

(a) Computed vortex sheet shape 2 body diameters downstream of wing trailing edge.

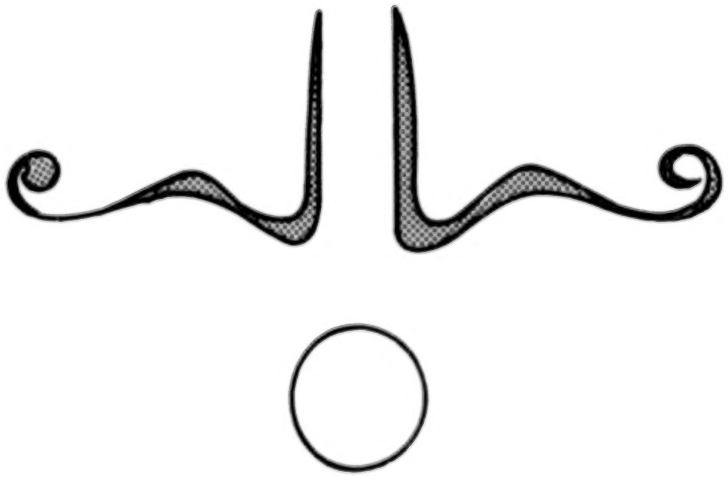

(b) Approximate form of developing vortex sheets 2 body diameters downstream of wing trailing edge as obtained from vapor screen photograph.

Figure 6.- Computed vortex sheet shape and corresponding vapor screen photograph of missile at $\alpha = 27^{o}$ and $M = 3.95$.

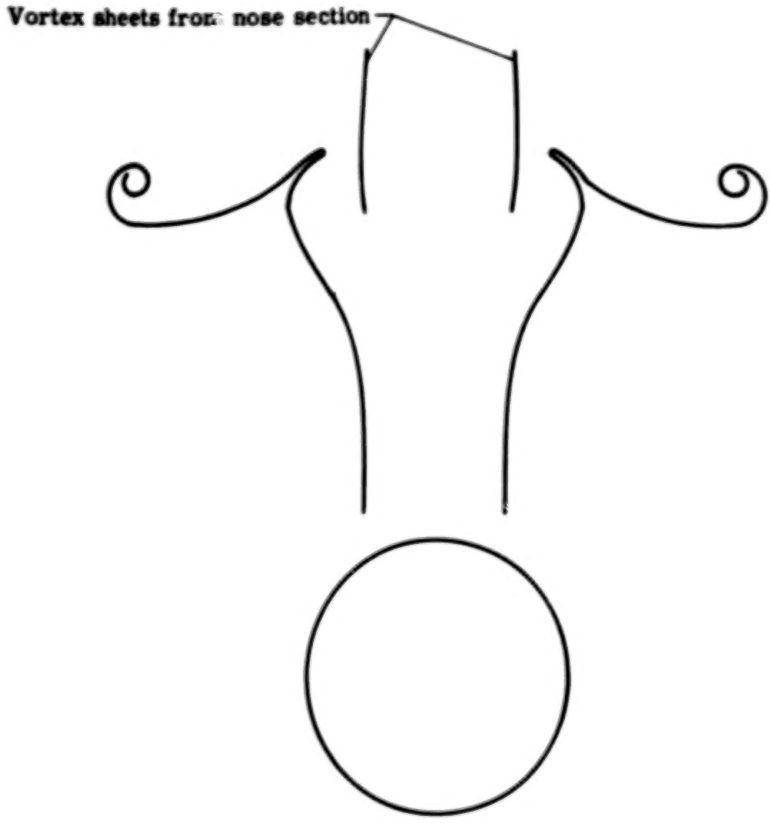

(a) Computed vortex sheet shape in cross-flow plane 5 body diameters downstream of wing trailing edge.

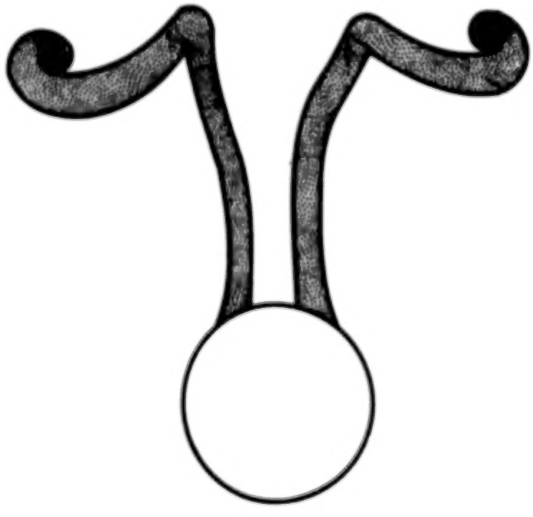

(b) Approximate form of developing vortex sheets 5 body diameters downstream of wing trailing edge as obtained from vapor screen photograph.

Figure 7.- Computed vortex sheet shape and corresponding vapor screen photograph of missile at $\alpha = 33^{\circ}$ and $M = 3.95$.

1. Report No. NASA TP-1183	2. Government Accession No.	3. Recipient's Catalog No.
4. Title and Subtitle A DISTRIBUTED VORTEX METHOD FOR COMPUTING THE VORTEX FIELD OF A MISSILE		5. Report Date June 1978 6. Performing Organization Code
7. Author(s) Raymond L. Barger		8. Performing Organization Report No. L-11963 10. Work Unit No. 505-11-23-03
9. Performing Organization Name and Address NASA Langley Research Center Hampton, VA 23665		11. Contract or Grant No. 13. Type of Report and Period Covered Technical Paper
12. Sponsoring Agency Name and Address National Aeronautics and Space Administration Washington, DC 20546		14. Sponsoring Agency Code

15. Supplementary Notes

16. Abstract

Vortex sheet development in the flow field of a missile was investigated by approximating the sheets in the cross-flow plane with short straight-line segments having distributed vorticity. In contrast with the method that represents the sheets as lines of discrete vortices, this distributed vortex method produced calculations with a high degree of computational stability.

17. Key Words (Suggested by Author(s))	18. Distribution Statement
Missile Flow field Vortices Body vortices Roll-up	Unclassified - Unlimited Subject Category 02

19. Security Classif. (of this report)	20. Security Classif. (of this page)	21. No. of Pages	22. Price*
Unclassified	Unclassified	16	$4.00

* For sale by the National Technical Information Service, Springfield, Virginia 22161

NASA-Langley, 1978